

PACS numbers: 42.65.Ky; 42.65.Jx; 42.65.Re; 52.38.Hb; 52.50.Jm
DOI: 10.1070/QE2015v045n05ABEH015773

Visible supercontinuum radiation of light bullets in the femtosecond filamentation of IR pulses in fused silica

S.V. Chekalin, V.O. Kompanets, A.E. Dokukina, A.E. Dormidonov, E.O. Smetanina, V.P. Kandidov

Abstract. **We report experimental and theoretical investigations of visible supercontinuum generation in the formation of light bullets in a filament produced by IR pulses. In the filamentation of a 1700–2200 nm pulse in fused silica, bright tracks are recorded resulting from the recombination glow of carriers in the laser plasma produced by a sequence of light bullets and from the scattering in silica of the visible supercontinuum generated by the light bullets. It is found that the formation of a light bullet is attended with an outburst of a certain portion of supercontinuum energy in the visible range. The energy outburst is the same for all bullets in the sequence and becomes smaller with increasing pulse wavelength.**

Keywords: *filamentation, femtosecond pulses, anomalous dispersion, plasma channels, light bullets.*

1. Introduction

Light bullets (LBs) result from the spatio-temporal compression of an optical wave packet. The conception of LB formation in the nonlinear-optical interaction of a wave packet and a dispersive medium with a cubic nonlinearity was first formulated by Silberberg [1] proceeding from an analysis of the quasi-optical equation in the aberrationless paraxial approximation [2]. For guiding structures with controllable dispersion and nonlinear properties, the pulse compression was investigated for planar waveguides [3–6] and photonic crystals [7]. In the volume of a transparent dielectric medium, the shortening of the duration of a high-intensity pulse was observed in the filamentation in atomic and molecular gases [8] with normal group velocity dispersion, as well as in noble-gas cells with optimisation of the pressure [9], pulse parameters [10] and filament length [11, 12]. The time delay of Kerr and plasma nonlinearity delays [13], a defocusing in laser-induced plasma [14] and the formation of an envelope shock at the trailing pulse edge [15] were considered as the physical models of light-pulse compression in the filamentation. In a dissipative nonlinear medium, the formation of LBs may result from continuous energy transfer to the central region of the wave packet to make up for the nonlinear loss [16].

S.V. Chekalin, V.O. Kompanets Institute of Spectroscopy, Russian Academy of Sciences, ul. Fizicheskaya 5, Troitsk, 142190 Moscow, Russia; e-mail: chekalin@isan.troitsk.ru;
A.E. Dokukina, A.E. Dormidonov, E.O. Smetanina, V.P. Kandidov Department of Physics and International Laser Centre, M.V. Lomonosov Moscow State University, Vorob'evy Gory, 119991 Moscow, Russia; e-mail: kandidov@physics.msu.ru

Received 29 January 2015; revision received 6 February 2015
Kvantovaya Elektronika **45** (5) 401–407 (2015)
Translated by E.N. Ragozin

The filamentation of femtosecond laser light is attended with a strong self-phase modulation of the light field and the consequential superbroadening of the frequency-angular spectrum [17], which opens the door to the efficient compression of a wave packet in space and time. The use of an external compressor after an argon cell, in which the spectrum was broadened in the filamentation, permitted shortening the pulse duration to several femtoseconds [18, 19].

When the group velocity exhibits anomalous dispersion, the function of a compressor is fulfilled directly by the propagation medium, in which a pulse is compressed in time in the self-phase modulation due to the Kerr nonlinearity. The feasibility of forming a quasi-periodic sequence of LBs in the filamentation in the conditions of anomalous group velocity dispersion was numerically studied by Bergé and Skupin [20], who gave a physical interpretation of the multiple collapse of high-power pulses recorded at a wavelength $\lambda = 1550$ nm in a BK7 glass sample [21]. The formation of a sequence of LBs in the pulse filamentation in the conditions of anomalous group velocity dispersion was numerically investigated in Ref. [22] and experimentally confirmed by autocorrelation measurements [23, 24]. The bullet of diameter 50 μm was equal to about two optical cycles in duration in the filamentation of a 1800-nm pulse in fused silica. The following bullets emerge due to energy transfer from the leading pulse edge in the self-phase modulation of the light field in the conditions of anomalous group velocity dispersion. Proceeding from the data on the spatio-temporal intensity distribution recorded in the filamentation of 1800 nm pulses in sapphire, Majus et al. [25] proposed a scenario, whereby an LB consists of a high-intensity core and a low-intensity periphery similar to a Bessel beam.

Our work is concerned with experimental and theoretical investigations of energy variations of the visible supercontinuum (visible SC) generated by LBs in the course of filamentation in fused silica, which take place under variations of pulse energy and near-to-medium IR wavelength tuning. We determined the main features of the transformation of the observed images of plasma channels (PCs) and luminous tracks in the filament, which are recorded by the recombination glow of the laser plasma and LB radiation scattering. The energy of visible SC generated by the LBs was shown to decrease with increasing wavelength of input pulses but was shown to be independent of the bullet position in the sequence.

2. Experimental facility

Our experimental research was carried out on the spectroscopic facility of the Joint Use Centre of the Institute of

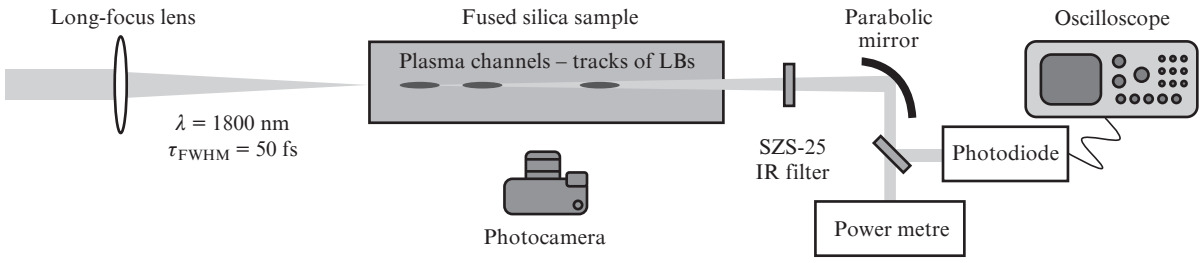

Figure 1. Schematic representation of experimental facility.

Spectroscopy, RAS. The experimental facility is schematised in Fig. 1. It comprised a Tsunami femtosecond oscillator (a Ti:sapphire laser) continuously pumped by a Millenia Vs solid-state laser, a Spitfire Pro regenerative amplifier pumped by an Empower 30 solid-state laser, and a TOPAS tunable parametric amplifier. Use was made of the pulses at wavelengths of 1700–2200 nm, which corresponded to the region of anomalous dispersion in fused silica. The FWHM duration of transform-limited λ = 1800 nm pulses was equal to 50 fs and their repetition rate was equal to 1 kHz; the pulse energy could be varied from 0.2 to 100 μJ using an NDC-100C-2 gradient attenuator.

The laser pulses were focused onto the input face of a 135-mm long fused silica sample with the use of a thin silica lens with a focal length F = 120 cm or a mirror with F = 50 cm. An ASF-20 autocorrelator (Avesta Project Ltd Company) was employed to measure the pulse duration. In the autocorrelation measurements of the duration of LBs, the paraxial part of a filament, in which the LBs were formed, was extracted with an aperture 50 μm in diameter, which was placed at the output face of the sample, and collected on the input autocorrelator window by a parabolic mirror. The pulse energy was measured by a Fieldmax sensor with a PS-10 detector as well as by a Thorlabs PDB-210A photodiode calibrated using the same sensor. The signal from the photodiode was delivered to an oscilloscope, which served to measure the energy of every pulse in the sequence at the output of the sample. In the measurement of visible SC energy in the 300–700 nm band, the output radiation was filtered by two 2-mm thick SZS-25 filters.

The images of PCs and luminous tracks in the filament were recorded respectively by the red recombination radiation of the laser plasma and the SC scattered in the sample through its lateral face with the use of a Canon EOS D800 digital camera. For a pulse repetition rate of 1 kHz, the exposure time was equal to 10 s; the camera ISO was 6400. The plasma luminescence does not exhibit directivity, and its contribution to the recorded SC spectrum is therefore negligible and could not be recorded by the spectrometer employed in our experiment.

3. Experimental results

The observation of PCs, whose occurrence is recorded by the characteristic red-pink carrier recombination glow, and of the luminous tracks of scattered SC (Fig. 2) revealed the following features. The glow of PCs emerged at the output face of a sample when the pulse energy exceeded some value, which depended on the wavelength and focusing conditions. No luminous tracks were observed until the occurrence of the first PC, whose length did not exceed several millimetres (Fig. 2, the lower lines). With increase in pulse energy, the PC became brighter and shorter, and in doing so it shifted in opposition to the direction of pulse propagation, towards the input face of the sample. In this case, in the direction of pulse propagation the PC originated a slightly diverging track, whose colouring depended on the filament-producing laser wavelength. For a wavelength λ = 1400 nm, the track acquired a yellow colour, for λ = 1800 nm a green colour, and a blue colour for λ = 2200 nm (Fig. 2). This variation of observed track colour is fully consistent with the existing notions about visible SC generation and LB formation.

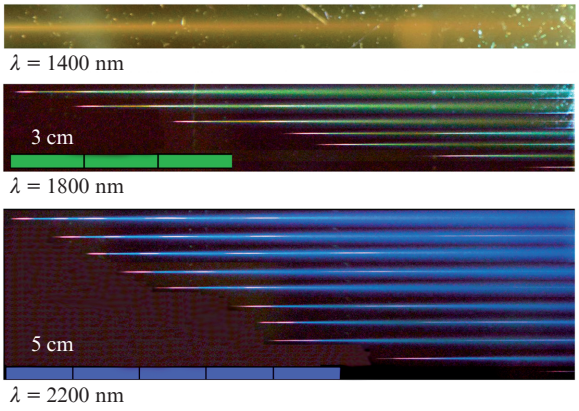

Figure 2. (Colour online) Images of PCs (red) and tracks of scattered visible SC, which is yellow in the filamentation of the λ = 1400 nm pulse, green for λ = 1800 nm, and blue for λ = 2200 nm. In the track photographs, the pulse energy increases from bottom to top from 12.3 to 17.2 μJ for λ = 1800 nm and from 37.8 to 56 μJ for λ = 2200 nm.

An LB is really a short-lived object with a high spatiotemporal localisation of the light field. In a strong LB field with an intensity of $\sim 10^{13}$ W cm^{-2}, in the medium there occurs production of a low-temperature laser plasma, whose recombination is recorded by the red glow of the PC. It is evident that the plasma is generated only during the LB lifetime, which is estimated from the PC length at several tens of picoseconds. The aberrational defocusing in the laser plasma, whose production is practically threshold-like for a high multiphoton order, is responsible for a sharp lowering of intensity in the resultant LB. The trailing edge of the LB with a strong temporal intensity gradient is the source of the anti-Stokes SC wing [26]. The steepness of the trailing edge of the pulse envelope depends only on the multiphoton order in the plasma production and rises with increase in the pulse wavelength

[27]. This in turn results in a significant short-wavelength shift of the visible radiation spectrum of the anti-Stokes SC wing generated by the LB.

The scattering of this SC in the sample is recorded in the form of a slightly diverging long coloured track; it ranges from the short PC, which is produced in the high-intensity LB formation [28], to practically the output face (Fig. 2).

Quite unexpected was the occurrence, inside of some of the observed tracks, of a considerably thinner and longer (over 3 cm) luminous fibre preceding the occurrence of the next PC and its related LB (Fig. 2, the first track from top for $\lambda = 1800$ nm, the second one from top for $\lambda = 2200$ nm). Unfortunately, the exposure of the recorded photographs ($\sim 10^4$ pulses) is too high to unambiguously document this event and accurately determine the fibre parameters. However, it is safe to say that the fibre is recorded only due to the scattering of the visible band of the anti-Stokes SC wing from the nonuniformity of refractive index induced by the light field. In this case, the field intensity is still below the threshold of the formation of a LB and, consequently, of a PC with a luminous plasma. The source of visible SC in this case is the preceding LB. This is why such a luminous fibre is not observed prior to the formation of the first PC: there is no source of SC, whose light could be scattered by the nonuniformity produced in the filament. However, it is pertinent to note that in luminescent media, like glasses, dye solutions, and air, visible glow may result from multiphoton absorption and the subsequent luminescence [29] in the propagation of a pulse in which a LB is not formed and the intensity remains below the laser plasma production threshold. In Ref. [30], such luminescent tracks were erroneously interpreted as long-lived LBs, whose duration remained invariable over a distance of several centimetres. According to the authors of Ref. 30, the medium was silica, which, as is well known, does not exhibit luminescence in the blue region, unlike glass. This is widely used in practice to distinguish it from glass.

An increase in pulse intensity prior to the emergence of an LB and plasma production in the medium is directly borne out by the following experiment. For a low intensity (below 10^{12} W cm^{-2}), on passing through the sample an input 50-fs long pulse ($\lambda = 1800$ nm) stretches to a 370-fs long duration owing to dispersion in silica, and its intensity becomes lower. On raising the input pulse energy to 2 μJ, the output pulse duration becomes shorter than 200 fs (the autocorrelation function was measured over the whole cross section of the beam). In this case, the divergence of the central part of the beam was recorded to increase. Prior to plasma production, with increasing input pulse power we observed a smooth growth of the energy fraction passing through a 50-μm diameter diaphragm at the sample output, which testified to the energy concentration on the beam axis, i.e. to the onset of filamentation (Fig. 3). Simultaneously, duration measurements of the pulse transmitted through the diaphragm revealed a shortening of the paraxial pulse duration to 50–90 fs. However, neither the occurrence of a PC nor the generation of a visible SC was observed in this pulse energy domain. This pulse propagation mode may be referred to as the spatio-temporal compression of a wave packet under a preplasma filamentation. On further increase in pulse energies we observed the simultaneous occurrence of a PC and a step-like rise of the signal corresponding to the visible SC energy; this was due the formation of the first LB

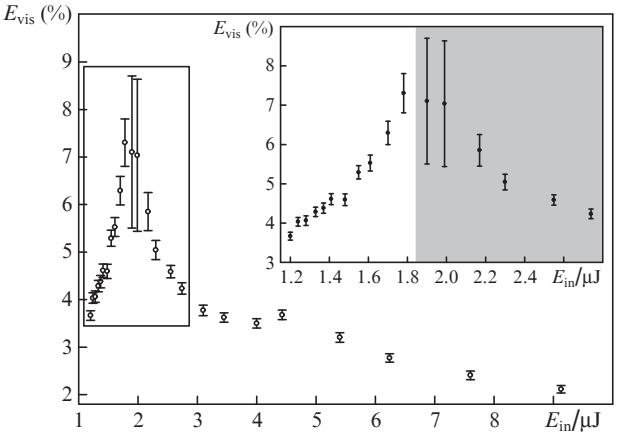

Figure 3. Energy fraction E_{vis} of the pulse transmitted through the diaphragm of diameter 50 μm at the sample output as a function of the energy E_{in} of the input $\lambda = 1800$ nm pulse. The inset is a blow-up of the same dependence in the 1.2–2.8 μJ pulse energy range; the domain where we observed visible SC generation is shown in grey.

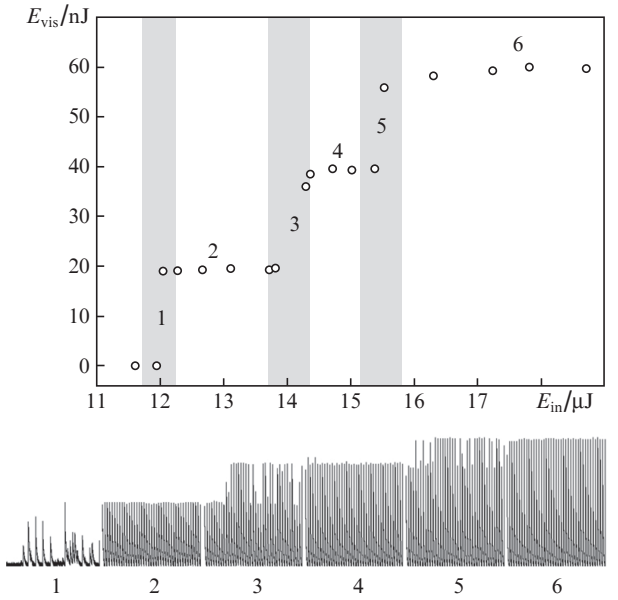

Figure 4. Dependence of visible SC energy E_{vis} on the input $\lambda = 1800$ nm pulse energy E_{in}. Bottom of drawing: oscilloscope traces of the signal from the photodiode, which measures the energy of each pulse in the visible domain. Domains 1, 3 and 5 denote the neighbourhoods (shown in grey) of the threshold energy values at which there emerge the 1st, 2nd, and 3rd PCs and respectively the 1st, 2nd, and 3rd LBs in the filament.

in the filament, which threshold-like in character (Fig. 4). In this case, with increasing pulse wavelength the threshold energy, at which the LB is formed (which is recorded by the occurrence of the first 'step') and hence the visible SC is generated, becomes higher, because the critical self-focusing power increases. The visible SC energy generated by the first LB is the same in the 1600–1900 nm domain, but it appreciable decreases for longer wavelengths owing to a higher absorption in the sample (Fig. 5).

For a pulse energy close the first LB formation threshold, the amplitude of photodiode signal exhibited strong pulse-to-pulse fluctuations in the measurement of visible SC energy

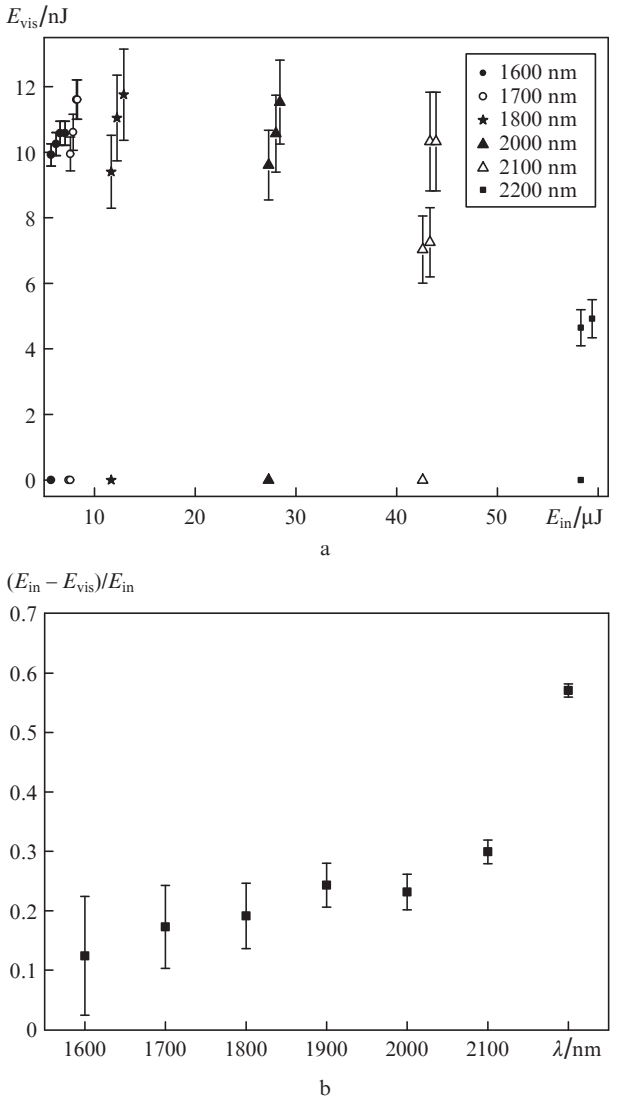

Figure 5. Step in the dependence of the visible SC energy E_{vis} on the incident pulse energy E_{in} on appearance of the first LB (see Fig. 4) (a) and fraction of the energy absorbed in the sample at different wavelengths (b).

(Fig. 4, domain 1). In this mode, the fraction of pulse energy transmitted through the 50-μm diameter diaphragm after the sample is close to its maximum and amounts to over 7% for the $\lambda = 1800$ nm pulse, when focused with a mirror with $F = 50$ cm (Fig. 3), and to ~6% when focused with long-focus lens. When the pulse energy exceeded the LB threshold formation, the visible SC energy remained invariable in a certain interval (Fig. 4, domain 2). In this case, the SC is produced by the single LB, which shifts to the input sample window with increasing pulse energy. Along with the obvious lowering of laser-to-visible SC conversion efficiency, also observed was a lowering of the relative pulse energy transmitted through the diaphragm 50 μm in diameter, which is due to the increase in beam divergence at the output sample face with displacement of the LB into the sample interior (Fig. 3). This lowering continued until the input pulse energy reached the next threshold, whereby the second LB appeared; it was recorded by the emergence of the next PC (Fig. 2) and the increase in the energy fraction transmitted through the diaphragm (Fig. 3, an energy of 4.4 μJ). In the formation of the second LB, the visible SC energy increased by nearly a factor of two in a stepwise manner (Fig. 4, domain 3).

A discrete increase in visible SC energy was repeated with the appearance of each next LB in the sequence. As a result, we observed steps in the dependences of SC energy on the input pulse energy. The steps, i.e. the domains of stable visible

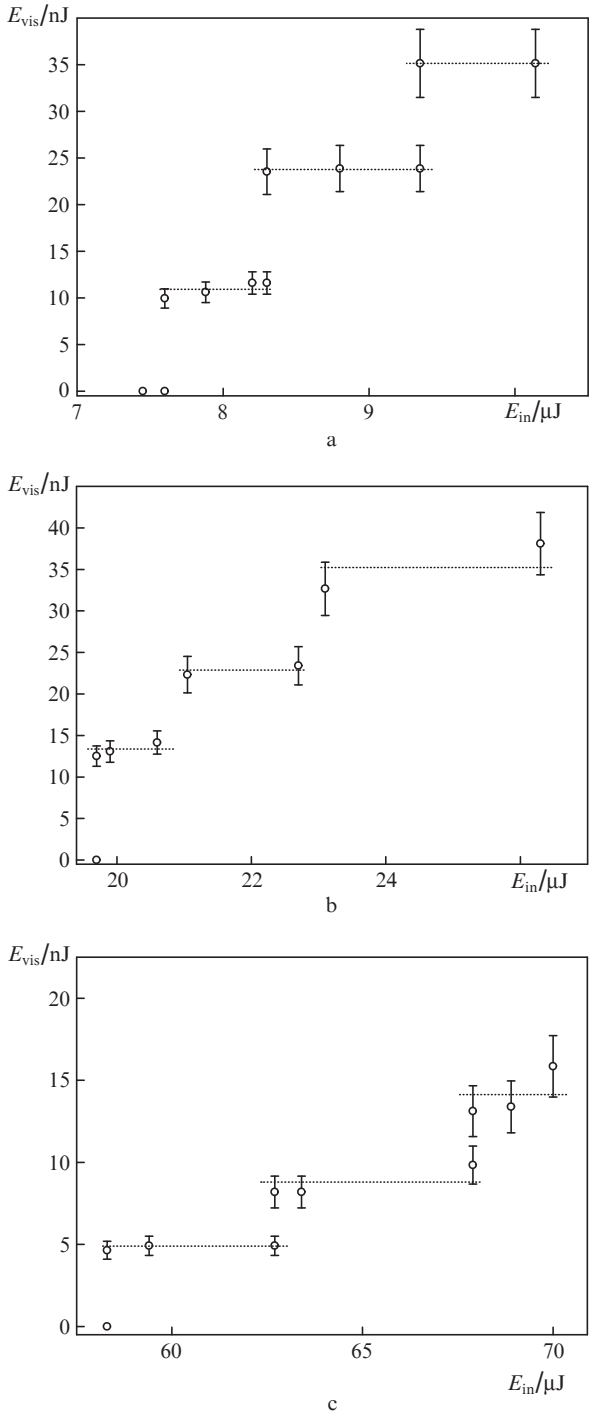

Figure 6. Variation of the visible SC energy E_{vis} in the $\lambda = 300-700$ nm domain with increasing energy E_{in} of the input pulse at wavelengths $\lambda =$ 1700 (a), 1900 (b), and 2200 nm (c).

SC energy, in which the pulse-to-pulse scatter of signal amplitudes is hardly present (Fig. 4, domain 6), correspond to the existence of a sequence with invariable number of LBs in the filament and, consequently, of coaxial PCs – one, two, three (Fig. 2). When the input energy was close to the threshold for the emergence of the next PC, we observed a transition mode, whereby the visible SC energy exhibited strong pulse-to-pulse variations (Fig. 4, domains 1, 3, and 5). This was due to the fluctuations of laser pulse energy, when the occurrence or absence of the next LB, and hence of the PC, was accidental. In our experiments we observed up to seven coaxial PCs; on further increase in energy, their formation mode became unstable, which was due to the strong effect of the fluctuations of laser light as well as to thermal distortions in the medium. An 'outburst' of visible SC energy was observed in the filamentation of laser pulses of different wavelength lying in the domain of anomalous group velocity dispersion (Fig. 6). In this case, the visible SC energy, which was generated by LBs, lowered with increase in input pulse wavelength but was independent of the LB position in the sequence.

The LB-to-SC conversion efficiency may be estimated from the following considerations. The phase modulation of the light field and the consequential pulse-driven visible SC generation develop in the paraxial filament region ~10 μm in diameter. According to the data of numerical simulations [27, 31], for the $\lambda = 1800$ nm pulse the SC energy fraction E_{vis} in the 300–1100 nm spectral range accounts for ~1.6% of its total energy E_{SC}. The visible SC energy fraction E_{vis} of the first step measured in our experiment for this wavelength is equal to ~0.1% of the incident energy E_{in}. On the other hand, the entire SC is formed in the filament or, more precisely, in the LB, whose energy E_{bul}, according to our measurements with the use a diaphragm 50 μm in diameter (Fig. 3), does not exceed 7% of E_{in}. Therefore, we have

$$E_{vis} \sim 10^{-3}E_{in} \sim 0.016E_{SC}, \quad E_{bul} \sim 7\times10^{-2}E_{in}.$$

By simple arithmetic operations we obtain $E_{bul} \sim E_{SC}$, i.e. the LB energy is close to the total SC energy in the spectral band. From this it easy to conclude that virtually all LB energy is converted to SC energy, which is the main cause of its dissipation and 'annihilation'.

4. Numerical simulations

Numerical investigations clearly illustrate the scenario of the formation of a sequence of LBs and PCs in the pulse filamentation under anomalous group velocity dispersion. Our simulations were performed in the slowly varying wave approximation [32]. In the formulation of the problem under consideration [22], it takes into account the diffraction and dispersion of a wave packet, its Kerr self-focusing, photo- and avalanche

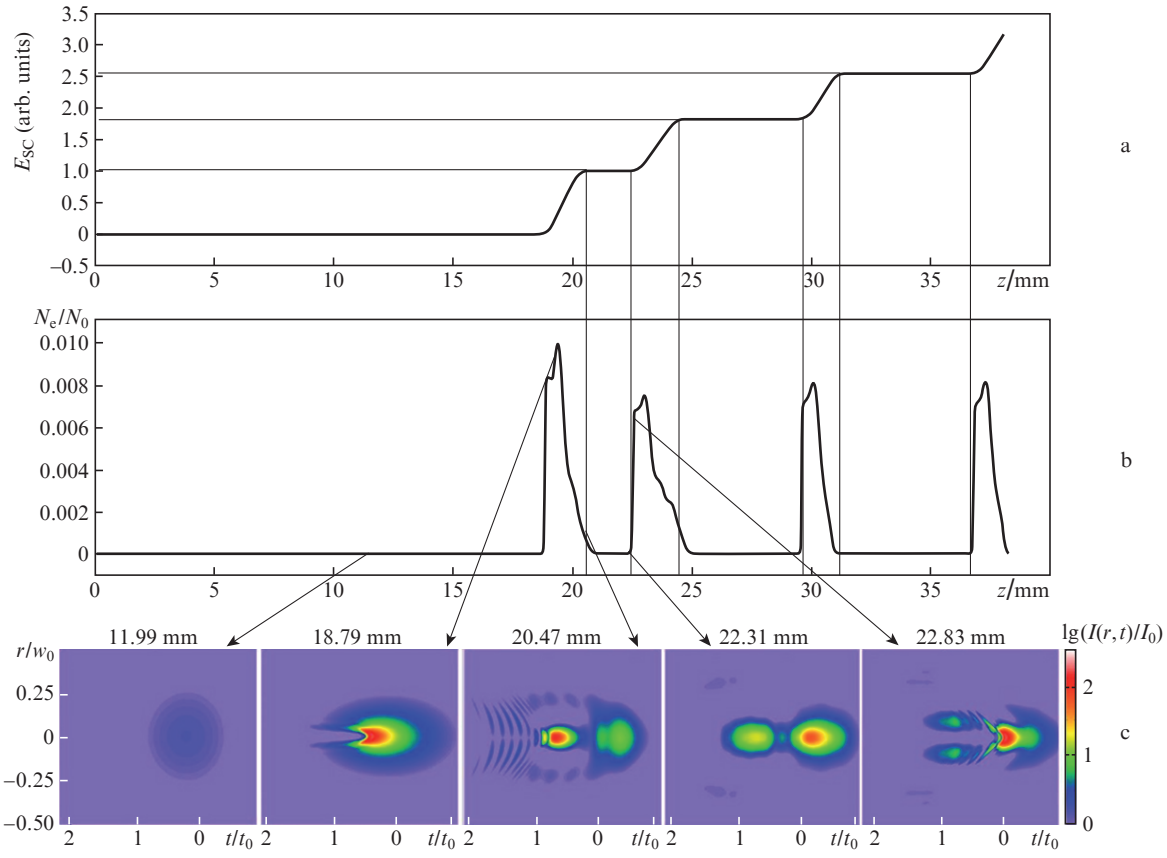

Figure 7. Visible SC energy $E_{vis}(z)$ (a) and on-axis electron density $N_e(z)/N_0$ (b) variations along the filament, where $N_0 = 2.1\times10^{22}$ cm^{-3} is the density of neutrals, and pseudo color patterns representing the spatio-temporal intensity distribution $I(r,t,z)/I_0$ for several positions along the filament (c). The parameters of the input pulse are as follows: a wavelength of 2200 nm, an energy of 10.8 μJ, a duration $2t_0 = 60$ fs (at a e^{-1} level), a beam radius $w_0 = 160$ μm, a peak intensity $I_0 = 2.5\times10^{11}$ W cm^{-2}, and the peak power is ten times the critical self-focusing power.

ionisation of the medium, the aberrational defocusing and absorption of the wave packet in the laser-induced plasma, as well as the effect of front self-steepening of the pulse envelope. In our numerical model, the silica dispersion was determined by the Sellmeier formula [33, 34] and the photoionisation rate by the Keldysh formula [35]. In our experiment, we employed weak focusing onto the input face of the sample (a nearly collimated beam), and so the shape of the transform-limited input pulse and intensity distribution at the cross section of the collimated beam were assumed to be Gaussian:

$$I(r,t,z=0) = I_0 \exp\left(-\frac{r^2}{w_0^2} - \frac{t^2}{t_0^2}\right).$$

In the numerical solution of the self-consistent nonlinear-optical problem, we determined the transformation of spatio-temporal light field intensity distribution $I(r,t,z)$ along the filament, the variation of electron density $N_e(z)$ on the PC axis, and the pulse spectrum energy $E_{vis}(z)$ in the visible band 500–1100 nm. Shown by way of example in Fig. 7 are the data obtained for the $\lambda = 2200$ nm pulses with parameters close to the experimental ones: an energy $E_{in} = 10.8$ μJ, a beam radius $W_0 = 160$ μm, and duration $2t_0 = 60$ fs (at a e^{-1} level), which corresponds to a FWHM duration of 50 fs. For the parameters involved, the peak intensity of the input pulse $I_0 = 2.5\times10^{11}$ W cm^{-2}, the peak power $P_0 = 201.6$ MW, and the ratio $P_0/P_{cr} = 10$, where $P_{cr} = 20.16$ MW is the critical self-focusing power for $\lambda = 2200$ nm in fused silica.

As is seen from the outlined results, along a filament there forms a sequence of PCs spaced at 5–10 mm. To each PC there corresponds a sharp increase in visible SC energy $E_{vis}(z)$, while the energy $E_{vis}(z)$ remains constant in the absence of a PC. PCs arise due to ionisation of the medium in a strong light field in the spatio-temporal compression of the wave packet. The increase in the electron density in the PC is virtually threshold-like, because the multiphoton ionisation order in fused silica for $\lambda = 2200$ nm is equal to 18. The intensity formed in the resultant LB amounts to 4×10^{13} W cm^{-2}, which is two orders of magnitude higher that the peak intensity I_0 of the input pulse. At the trailing edge of the wave packet there occurs aberrational defocusing in the laser-induced plasma, with the consequential strong increase in temporal intensity gradient. The visible SC energy accumulates with distance, because it is generated throughout the interval in which there exists an LB with a high field gradient. Subsequently the LB dissipates, and the next LB originates at the leading pulse edge with increase in light field intensity due to the temporal pulse compression under the Kerr phase modulation and anomalous group velocity dispersion. Therefore, in the filament there forms a sequence of high-intensity short-lived LBs, which generate the visible SC and are experimentally recorded by plasma recombination glow. In the interval between the LBs in the sequence, the field intensity is low and the visible SC energy does not change with distance. That is why there forms a sequence of steps in the variation of visible SC energy with distance, which is consistent with experimental data.

5. Conclusions

The formation of an LB in a femtosecond filament is attended with the ejection of a certain portion of visible SC energy. The dependence of the visible SC energy on the irradiating pulse energy has a characteristic ladder-like form, the emergence of each next step being due to the production of the next LB in the filament. Each LB of the sequence ejects the same visible SC energy, which becomes lower with increase in wavelength of the filament-producing light. In filamentation experiments in fused silica, the formation of an LB in the filament is recorded by the emergence of recombination glow of the laser plasma induced by a high-intensity LB and by the step of visible SC energy. The visible SC generated by the LB is visually recorded by its scattering in its propagation along the filament. The threshold energy of the pulse which gives rise to the first LB depends on the focusing conditions and increases with its wavelength. Proceeding from the resultant experimental data as well as from earlier spectral measurements, it is valid to conclude that the energy of LBs is almost completely transformed to the SC energy in its entire spectral band and that this is the main channel of LB dissipation.

Acknowledgements. This work was supported by the Russian Foundation for Basic Research (Grant No. 14-22-02025-ofi-m) and the RF President's Grants Council (State Support to Leading Scientific Schools Programme, Grant No. NSh-3796.2014.2).

References

1. Silberberg Y. *Opt. Lett.*, **15**, 1282 (1990).
2. Akhmanov S.A., Sukhorukov A.P., Khokhlov R.V. *Usp. Fiz. Nauk*, **93** (1), 19 (1967) [*Sov. Phys. Usp.*, **10** (5), 609 (1968)].
3. Fibich G., Ilan B. *Opt. Lett.*, **29**, 887 (2004).
4. Lobanov V.E., Kartashov Y.V., Torner L. *Phys. Rev. Lett.*, **105**, 033901 (2010).
5. Minardi S. et al. *Phys. Rev. Lett.*, **105**, 263901 (2010).
6. Eilenberger F. et al. *Phys. Rev. A*, **84**, 013836 (2011).
7. Mihalache D. et al. *Phys. Rev. E*, **70**, 055603(R) (2004).
8. Koprinkov G. et al. *Phys. Rev. Lett.*, **84**, 3847 (2000).
9. Stibenz G., Zhavoronkov N., Steinmeyer G. *Opt. Lett.*, **31**, 274 (2006).
10. Skupin St. et al. *Phys. Rev. E*, **74**, 056604 (2006).
11. Uryupina D. et al. *J. Opt. Soc. Am. B*, **27**, 667 (2010).
12. Brée C., Demircan A., Steinmeyer G. *Phys. Rev. A*, **83**, 043803 (2011).
13. Couairon A. *Eur. Phys. J. D*, **27**, 159 (2003).
14. Berge L., Skupin S. *Phys. Rev. Lett.*, **100**, 113902 (2008).
15. Gaeta A.L. *Phys. Rev. Lett.*, **84**, 3582 (2000).
16. Porras M., Parola A., Trapani P. *J. Opt. Soc. Am. B*, **22**, 1406 (2005).
17. Kandidov V.P. et al. *Appl. Phys. B*, **77**, 149 (2003).
18. Hauri C.P. et al. *Appl. Phys. B*, **79**, 673 (2004).
19. Xiaowei Chen et al. *Opt. Lett.*, **32**, 2402 (2007).
20. Bergé L., Skupin S. *Phys. Rev. E*, **71**, 065601(R) (2005).
21. Moll K.D., Gaeta A. *Opt. Lett.*, **29**, 995 (2004).
22. Smetanina E.O., Dormidonov A.E., Kandidov V.P. *Laser Phys.*, **22**, 1189 (2012).
23. Smetanina E.O. et al. *Laser Phys. Lett.*, **10**, 105401 (2013).
24. Chekalin S.V. et al. *Kvantovaya Elektron.*, **43** (4), 326 (2013) [*Quantum Electron.*, **43** (4), 326 (2013)].
25. Majus G. et al. *Phys. Rev. Lett.*, **112**, 193901 (2014).
26. Smetanina E.O. et al. *Kvantovaya Elektron.*, **42** (10), 913 (2012) [*Quantum Electron.*, **42** (10), 913 (2012)].
27. Smetanina E.O. et al. *Kvantovaya Elektron.*, **42** (10), 920 (2012) [*Quantum Electron.*, **42** (10), 920 (2012)].
28. Chekalin S.V. et al. *Program 23st Int. Laser Physics Workshop* (Sofia, Bulgaria, 2014) rep. 5.4.7, p. 35.
29. Schroeder H., Chin S.L. *Opt. Commun.*, **234**, 399 (2004).
30. Durand M. et al. *Phys. Rev. Lett.*, **110**, 115003 (2013).

31. Smetanina E.O. et al. *Opt. Lett*., **38**, 16 (2013).
32. Brabec T., Krausz F. *Phys. Rev. Lett.*, **78**, 3282 (1997).
33. Malitson I.H. *J. Opt. Soc. Am*., **55**, 1205 (1965).
34. Sellmeier W. *Annalen der Physik und Chemie*, **219**, 272 (1871).
35. Keldysh L.V. *Zh. Eksp. Teor. Fiz*., **47**, 1945 (1964) [*JETP*, **20** (5), 1307 (1965)].